CERN-ACC-NOTE-2019-0022

2019.06.17
marco.d'andrea@cern.ch

Crystal Collimation Tests with Proton Beams

M. D'Andrea, D. Mirarchi, S. Redaelli, B. Salvachua Ferrando, L. Nevay, R. Rossi, W. Scandale, S. Montesano, F. Galluccio, P. Serrano Galvez, C. Dionisio Barreto, M. Butcher, I. Lamas Garcia
CERN, Geneva, Switzerland

Keywords: LHC, collimation, crystal, UA9

Summary

During MD3327, performed in two steps on June 14$^{\text{th}}$ and July 27$^{\text{th}}$ 2018, silicon crystals for a crystal-assisted collimation system were tested, with particular focus on the newly installed crystal on the horizontal plane of Beam 2. Crystal collimation is studied as an alternative scheme for ion collimation at the HL-LHC. Tests with proton beams are fundamental to perform the initial setup of the system in preparation of the ion run 2018.

1 Introduction

The crystal collimation concept relies on the usage of bent crystals that can deflect halo particles at large angles of up to tens of μrad, as opposed to the standard LHC multi-stage collimation where an amorphous primary collimator scatters halo particles at a few μrad onto several secondary collimators. Crystal primaries could in principle send halo particles coherently onto a single absorber. A setup that uses only existing secondary collimators as absorbers for the channeled beam has been conceived for crystal collimation beam tests in IR7 [1]. Between 2015 and 2017, four bent crystals were installed in IR7, one for each cleaning plane on both Beam 1 and Beam 2. During the years, these crystals were tested and channeling was successfully observed at injection and top energy for both proton and ion beams. However, due to non-optimal results observed for B2H [2, 3], a new strip crystal was installed on Beam 2 during EYETS2017. The main goal of this MD was to check the performances of the new hardware, as well as to check the stability of the hardware and settings for previously installed crystals. These operations are crucial to have early feedback on the hardware in preparation for the 2018 ion run. A first MD was granted in MD block 1, but the full program could not be completed due to limited machine availability for causes independent of MD operations. The rest of the program was postponed to MD block 2, but

issues with the orbit correctors during the ramp limited the measurements that could be performed at top energy. A total of 16 hours were allocated for the two MDs (originally 6 hours per MD, extended to 8 hours), but only a total of 6 hours were used for measurements (not including setting up and energy ramps).

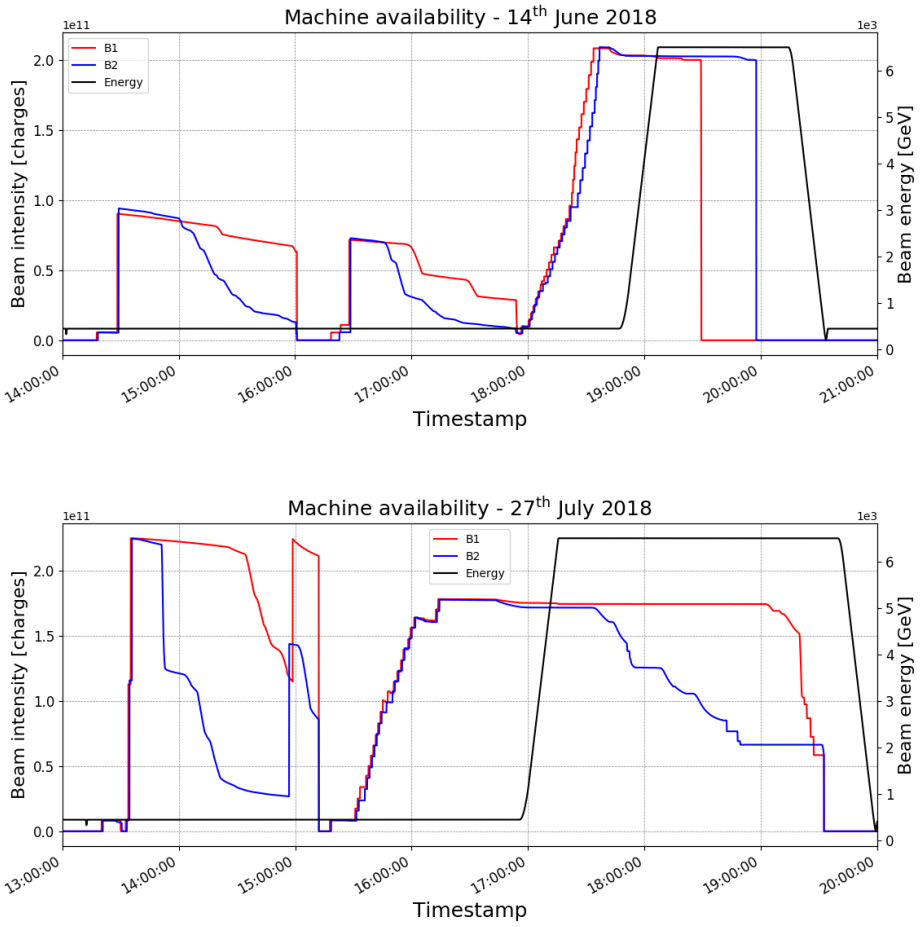

Figure 1: Beam 1 and Beam 2 intensity and energy during the first (top) and second (bottom) MD slot.

2 Beam Setup

The MD was performed using several low-intensity bunches at both injection and flat top energy with standard 2018 optics for both Beam 1 and Beam 2, in a configuration that was extensively tested in previous crystal MDs [2–6]. The transverse dumper (ADT) was used to excite the beam with white noise, as in standard collimation loss maps, to achieve controlled primary beam losses on crystals and/or collimators. To have enough losses for the time needed to complete measurements such as angular scans, the ADT window was enlarged to act on three different bunches. This allows to achieve sufficiently high loss rates for longer times. For this reason, the filling scheme consisted of 3-pilot trains with 2 μs

spacing between each train and 3 μs spacing between each bunch. For machine protection reasons, up to 30 bunches with total intensity below $3 \cdot 10^{11}$ protons are allowed at flat top. At injection nominal bunches can be used respecting the limit of $5 \cdot 10^{11}$ protons.

The scheduled measurements involved the following main activities:

1. beam-based alignment of the crystal with respect to the beam orbit and transverse positioning as primary collimator;
2. angular scan to find the optimal channeling condition;
3. transverse scan of the channeled beam with a secondary collimator;
4. cleaning measurements through loss maps with the crystal in channeling position.

Fig. 1 shows the intensity and energy of the beams during the MD slots. Only a small fraction of the program. Angular scans were performed at injection with B1H, B1V and B2H, as well as a linear scan with B2H. On the other hand, only a quick angular scan with B2H was performed at flat top and cleaning measurements had to be completely dropped.

Part of the remaining program was carried out during MD block 2. Measurements at injection were very efficient and both angular and linear scans were performed for the horizontal crystals. During the ramp, a trip of several power converters of orbit correctors affected Beam 2, making impossible to perform reliable measurements for the B2H crystal. A small set of loss maps on B1H was nonetheless performed.

3 MD Block 1

3.1 Beam 1 at Injection Energy

Due to the limited time available, measurements with Beam 1 crystals were carried out only at injection energy in the first block. Only angular scans to re-establish the optimal channeling orientation were performed and the results are shown in Fig. 2. The measured reduction factor of local losses at the crystal was 18.3 for B1H and 30.0 for B1V, both consistent with the results of previous years [3, 4, 6]. The Beam 1 layout was unchanged since the first installation in 2015 and these measurement will be used for assessing the reproducibility of the system.

3.2 Beam 2 at Injection Energy

Due to time constraints, all measurements with Beam 2 were focused on the newly installed B2H crystal, with which both angular and linear scans were performed at injection energy. Fig. 3 shows the BLM signals of all TCSGs and TCLAs in IR7 during the angular scan. Even though the BLM readout at the absorber shows a considereably lower than expected reduction factor [2, 3], the signature of the interaction with the crystal can be clearly seen from these plots. In particular, the TCSG.6L7.B2 and the TCLAs capture the deflected beam in volume reflection regime, showing a higher signal in this condition. On the other

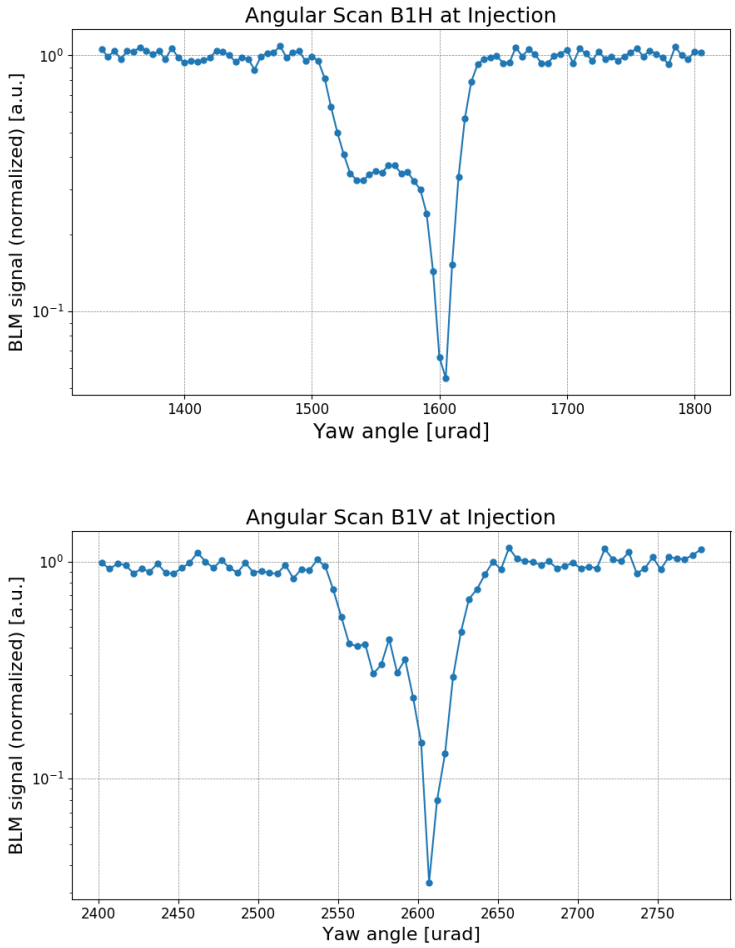

Figure 2: Angular scan on Beam 1 at injection energy with the horizontal (top) and vertical (bottom) crystal (first MD block). The BLM signal has been normalized to the particle flux and to the amorphous level.

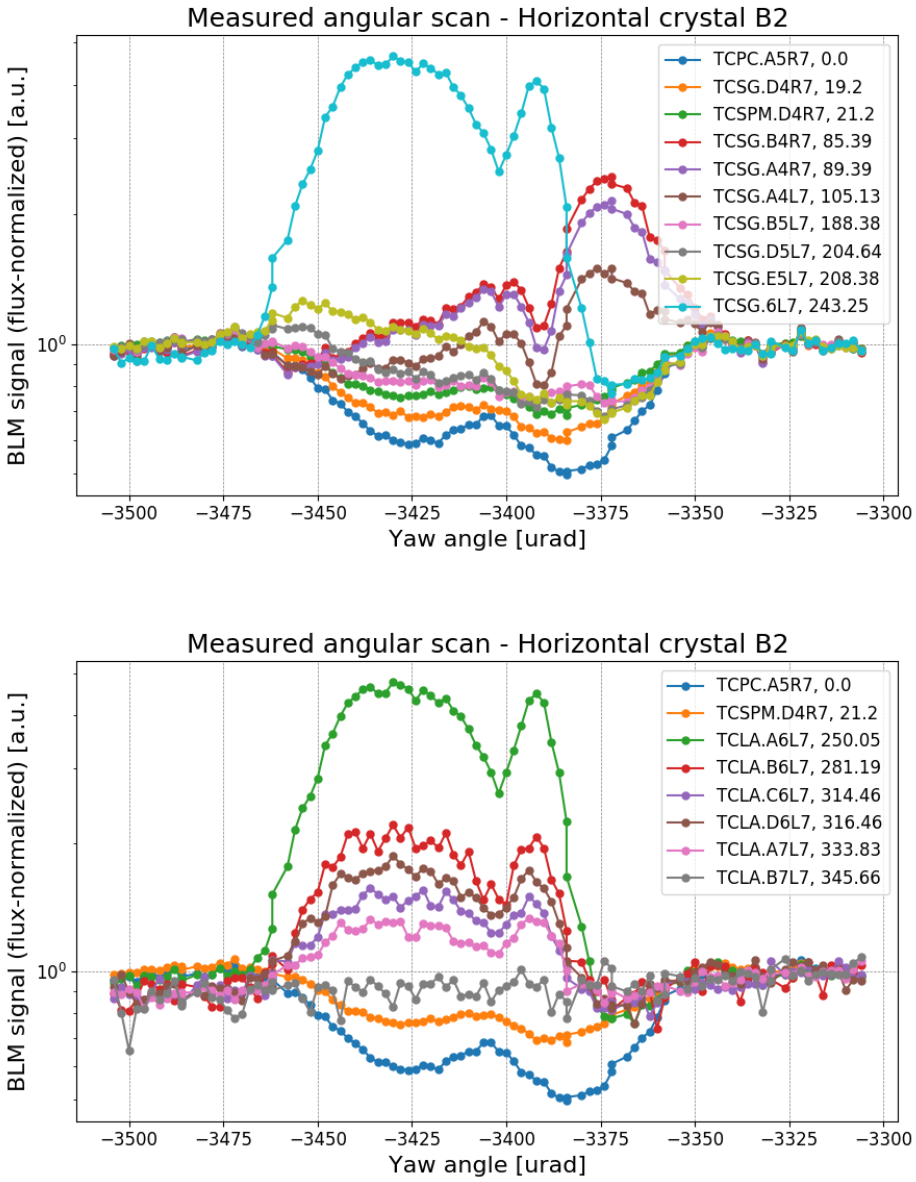

Figure 3: BLM signal of all the TCSGs (top) and TCLAs (bottom) in IR7 during the angular scan with B2H at injection energy (first MD block). The signals have been normalized to the beam flux and to the amorphous level.

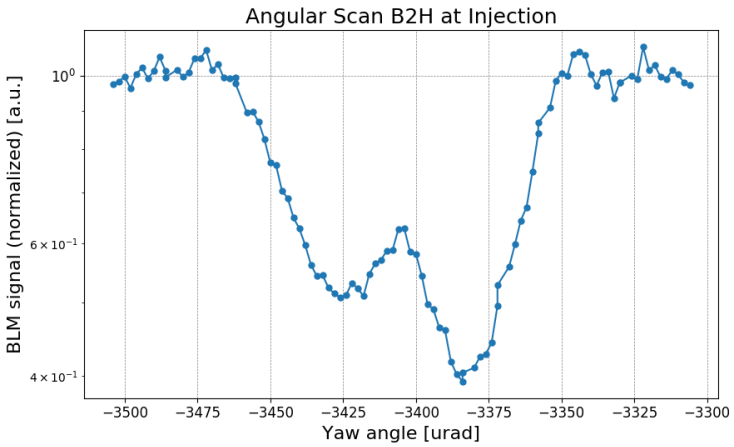

(a) Angular scan: normalized losses at the absorber as a function of the crystal angle.

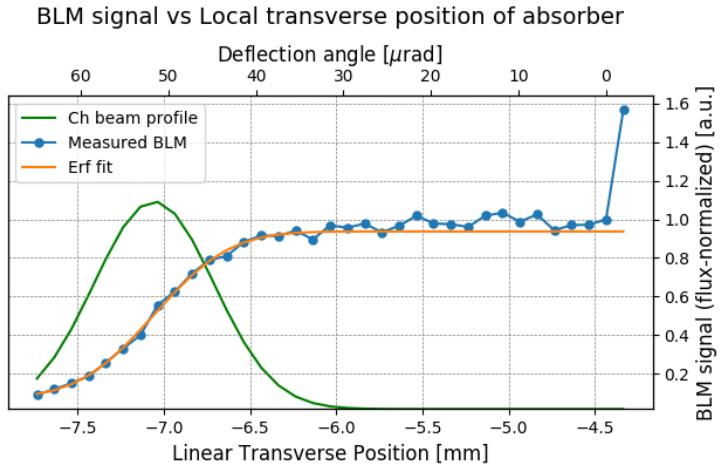

(b) Linear scan: normalized losses at the absorber as a function of its linear transverse position. An error function fit has been performed to estimate the deflection angle of the channeled beam.

Figure 4: Angular (top) and linear (bottom) scan on Beam 2 at injection energy with the horizontal crystal (first MD block).

hand, the other TCSGs are in the shadow of the TCSG.B4R7.B1 (i.e. the primary absorber) and have a higher signal when the crystal is in channeling orientation.

Fig. 4 shows the signal of the crystal BLM during the angular and linear scan. The angular scan shows a reduction factor of local losses at the crystal of 2.5, which is lower than expected as previously mentioned, and an unusual shape without a distinguishable volume reflection plateau. Furthermore, the signal at the TCSG.6L7.B2 in volume reflection is higher than expected, with respect to the signals of the other secondaries when in channeling.

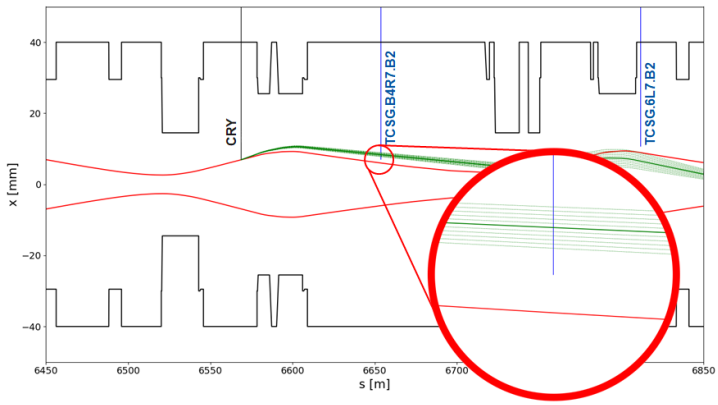

(a) Crystal at 5.7 σ

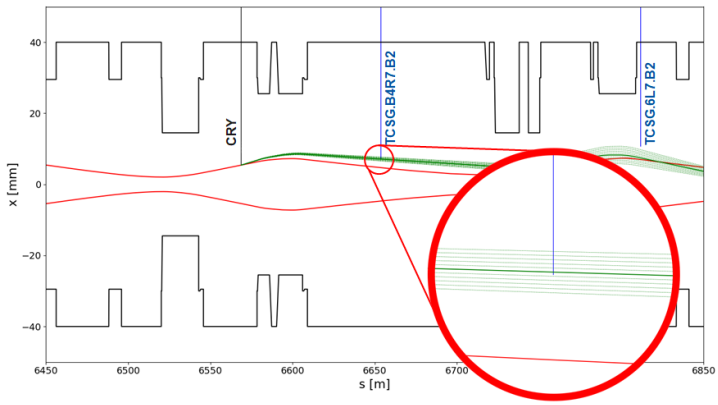

(b) Crystal at 4.46 σ

Figure 5: Trajectory of the channeled beam on the horizontal plane with a zoom-in at the location of the absorber (TCSG.B4R7.B2). The plots show the machine aperture (red), the beam envelope at the crystal aperture (red), the deflected beam (solid green) and a scan of possible trajectory with different crystal bending angles (dashed green, up to ± 10 μrad with respect to the measured bending).

This behaviour can be explained by a non-optimal alignment of the crystal during the initial setup. The crystal was intended to be aligned with the primary collimators at 5.7 σ, but it was instead closed further because the blow up of the beam was accidentally not started during the first steps of the beam-based alignment. A comparison of the transverse position of the absorber when it intercepted the primary beam during the linear scan and the

expected beam width at 5.7 σ showed that the crystal was actually placed at an aperture of 4.46 σ. As can be seen in Fig. 5, in this configuration the TCSG.B4R7.B2 collimator used as absorber does not completely intercept the channeled beam. As such, a fraction of the channeled particles continues its path along the machine and eventually hits the crystal again, and the deflected beam travels closer to the TCSG.6L7.B2, explaining the higher signal.

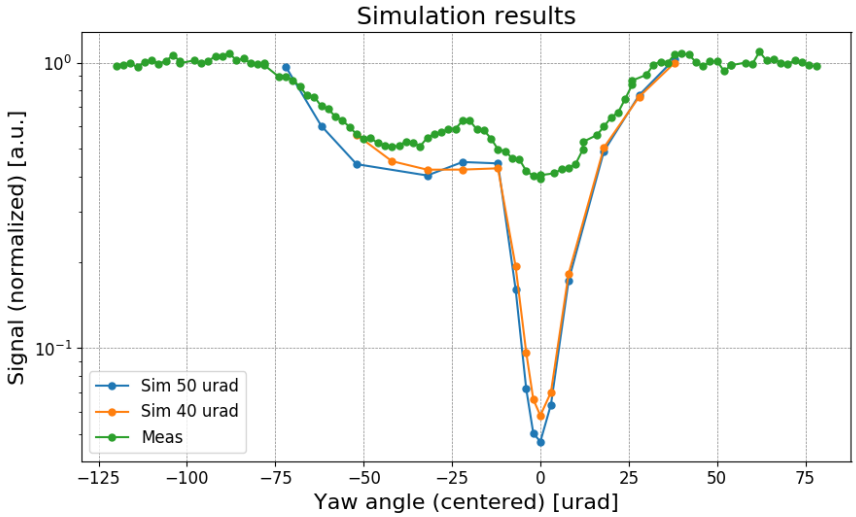

Figure 6: Comparison of measured B2H angular scan at injection with simulations with a crystal bending angle of 50 and 40 μrad respectively (first MD block). The values are normalized to the amorphous level.

The bending angle of the crystal (i.e. the deflection given to the channeled halo) can be estimated from the linear scan of the secondary collimator. Assuming that the crystal was placed at 5.7 σ as originally intended, this yields a bending angle close to 40 μrad, far from the required specifics of 50±5 μrad. However, with the crystal set at 4.46 σ instead, as previously discussed, the estimated becomes 47 μrad. Fig. 6 show a comparison of the measured angular scan with simulations for both of the estimated bending angles. Keeping in mind that this is only a qualitative comparison, as further simulation steps are required to precisely reconstruct the BLM signal, the shape of the angular scan is closer to the one obtained by simulating a crystal with a 50 μrad bending angle rather than a 40 μrad bending angle, including the absence of the volume reflection plateau.

3.3 Beam 2 at Flat Top Energy

Only a fast angular scan was performed with B2H at top energy. This was meant to be just the first scan to re-establish the optimal channeling orientation found at injection after the energy ramp, but the beam was dumped shortly afterwards because cryogenic conditions were lost in IR4, so no more data were collected. Fig. 7 shows the BLM signals of all TCSGs and TCLAs in IR7 during the angular scan. Compared to injection, the shaped of the well the reduction of losses at the absorber in channeling condition is much more

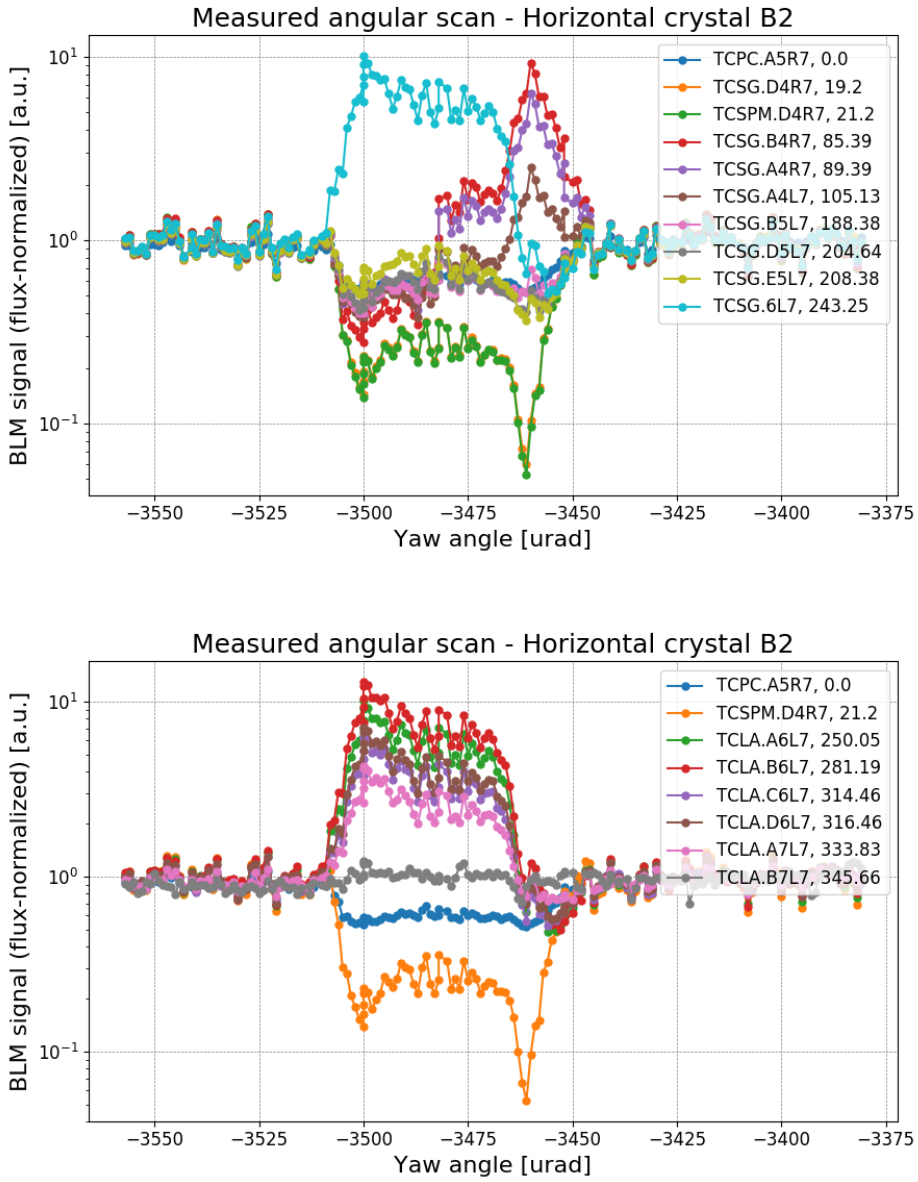

Figure 7: BLM signal of all the TCSGs (top) and TCLAs (bottom) in IR7 during the angular scan with B2H at injection energy (first MD block). The signals have been normalized to the beam flux and to the amorphous level.

in line with expectations [2, 3], indicating that no issues with the alignment where present at flat top. During the online analysis, the readout at the crystal was not clear enough to precisely identify the channeling orientation, so the signal from the TCSPM.D4R7.B2 was used instead.

After subtracting the background noise, the reduction factor of local losses at the crystal could be measured with the crystal BLM, resulting in 16.9. However, as can be seen in Fig. 8 where the scan is compared with simulations, the shape of the angular scan is quite narrow, suggesting a bending angle closer to 40 μrad in contrast with what was observed at injection. This result has yet to be understood and these measurements have been repeated in subsequent MDs.

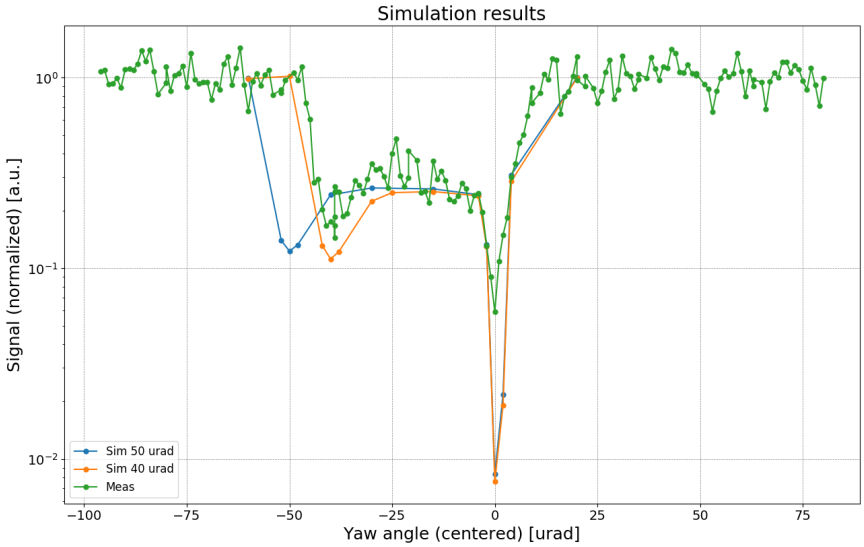

Figure 8: Comparison of measured B2H angular scan at top energy with simulations with a crystal bending angle of 50 and 40 μrad respectively (first MD block). The values are normalized to the amorphous level.

4 MD Block 2

4.1 Beam 1 at Injection Energy

During the second block, both angular and linear scans were performed at injection with the horizontal crystal. Both of them are shown in Fig. 9. The results of the angular scan are consistent with what was found in the first block, with a reduction factor of 21.6. The analysis of the linear scan yields a bending angle of 57.7 μrad, which is consistent with the results of previous years [3, 5, 6].

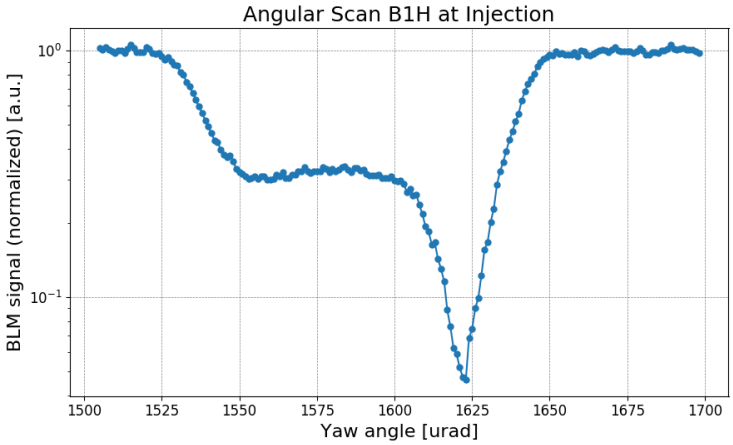

(a) Angular scan: normalized losses at the absorber as a function of the crystal angle.

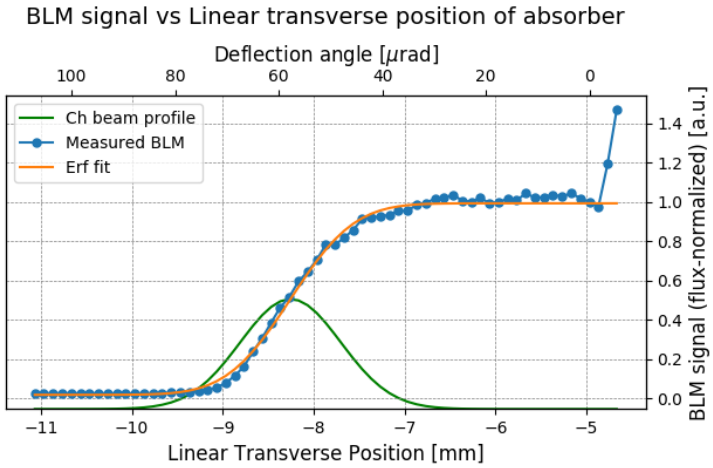

(b) Linear scan: normalized losses at the absorber as a function of its linear transverse position. An error function fit has been performed to estimate the deflection angle of the channeled beam.

Figure 9: Angular (top) and linear (bottom) scan on Beam 1 at injection energy with the horizontal crystal (second MD block).

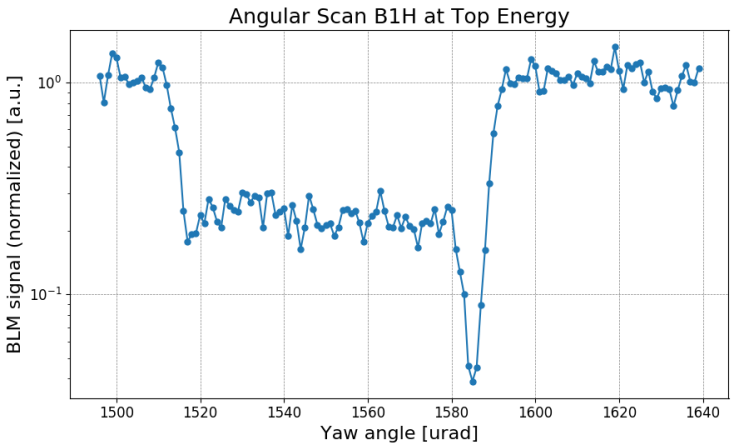

(a) Angular scan: normalized losses at the absorber as a function of the crystal angle.

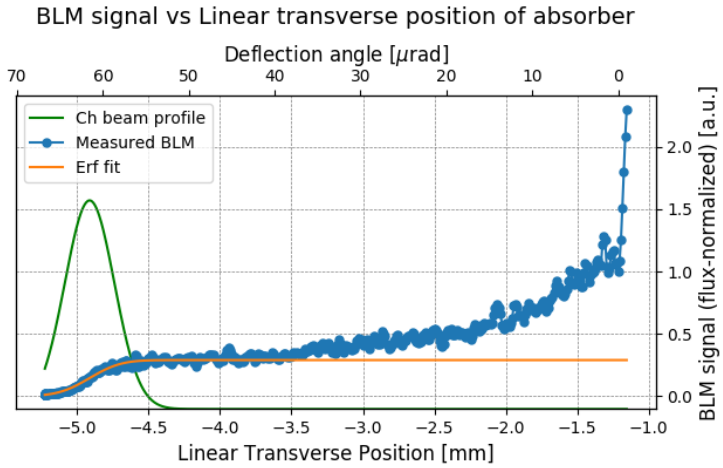

(b) Linear scan: normalized losses at the absorber as a function of its linear transverse position. An error function fit has been performed to estimate the deflection angle of the channeled beam.

Figure 10: Angular (top) and linear (bottom) scan on Beam 1 at flat top energy with the horizontal crystal (second MD block).

4.2 Beam 1 at Flat Top Energy

Angular and linear scans with the horizontal crystal at flat top are shown in Fig. 10. The estimated reduction factor of 25.8 and bending angle of 61.6 μrad are consistent with previous measurements [3, 4, 6].

Loss maps were performed with different settings of the TCLAs in IR7, i.e. at nominal, 8 σ and 6.5 σ aperture respectively, both for the standard and crystal collimation system. Losses are normalized to the lost particle flux in order to compare the IR7 leakage of the two systems. The cold region of IR7 is divided into three areas, each identified by the quadrupoles it includes (i.e. Q7, Q8-9 and Q10-11 respectively). The leakage ratio between the standard system is calculated for each area and shown in Fig. 11. These preliminary results show an improvement of up to a factor 4-5 in the Q8-9 and Q10-11 region. The working hypothesis for the higher losses on Q7 with crystals attributes them to showers from upstream collimators. In fact, the single pass dispersion at Q7 is still too low to induce dispersive losses, and these BLMs are very close to TCLAs that have higher loads when crystals are deployed. Detailed studies to confirm this hypothesis by means of energy deposition simulations are currently on-going.

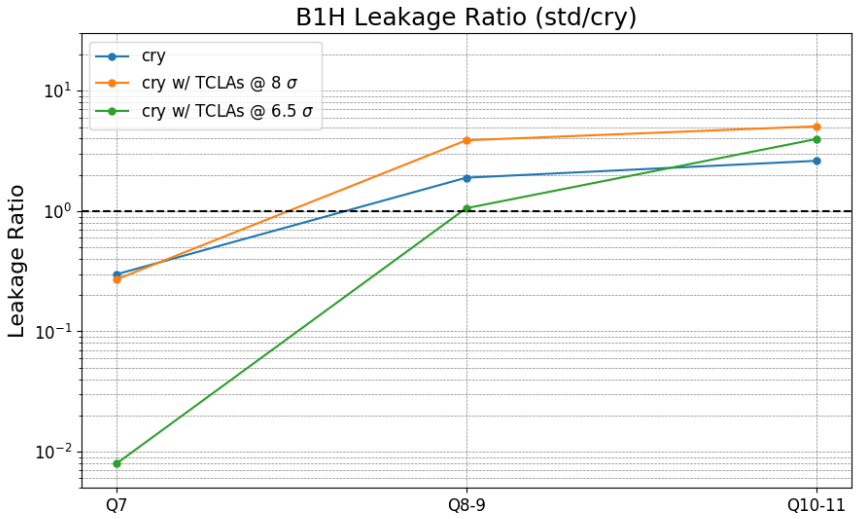

Figure 11: Ratio between losses measured for B1H using standard and crystal collimation systems for each area of the IR7 cold region and for each TCLAs configuration. A ratio higher than 1 indicates and improvement when crystals are deployed.

4.3 Beam 2 at Injection Energy

Measurements with the horizontal Beam 2 crystal were repeated during the second MD block. The angular and the linear scans are shown in Fig. 12. The angular scan yields a 13.0 reduction factor, which is in line with what was observed for the other crystals. However, the bending angle estimated from the linear scan is 43.2 μrad, significantly smaller than the

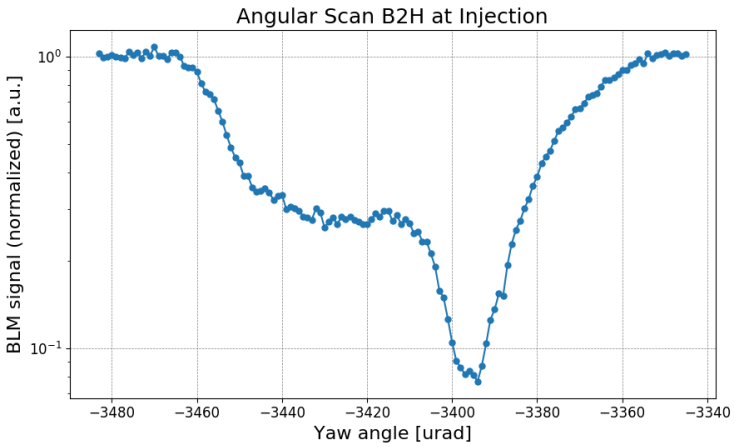

(a) Angular scan: normalized losses at the absorber as a function of the crystal angle.

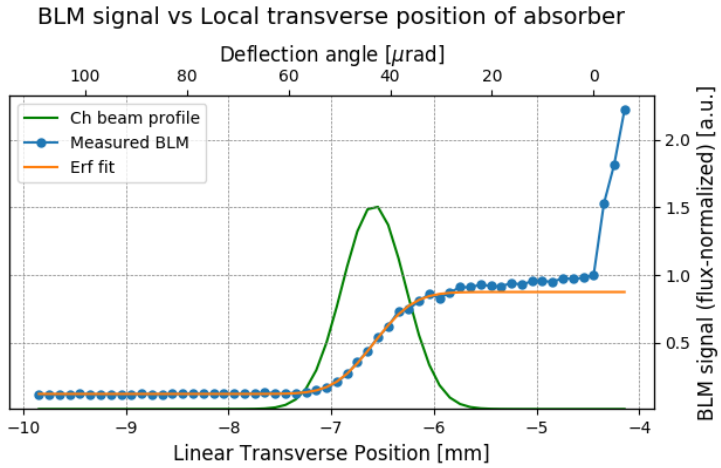

(b) Linear scan: normalized losses at the absorber as a function of its linear transverse position. An error function fit has been performed to estimate the deflection angle of the channeled beam.

Figure 12: Angular (top) and linear (bottom) scan on Beam 2 at injection energy with the horizontal crystal (second MD block).

valued measured during the first MD block and than the required specifics. This results is supported by simulations, as shown in Fig. 13.

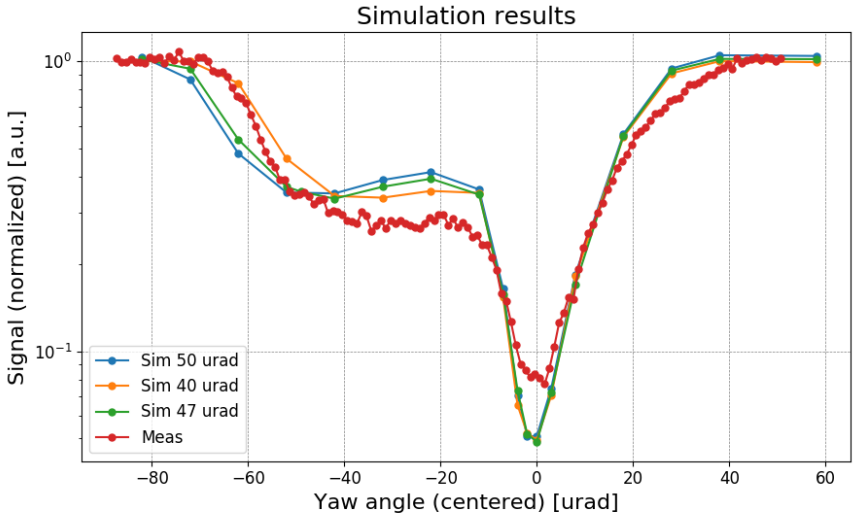

Figure 13: Comparison of measured B2H angular scan at injection with simulations with a crystal bending angle of 50, 47 and 40 μrad respectively (second MD block). The values are normalized to the amorphous level.

4.4 Beam 2 at Flat Top Energy

The same measurements were performed at flat top energy with the horizontal crystal on Beam 2. Fig. 14 shows the results of the angular and linear scans, which confirm what emerged from the first block. The reduction factor of local losses at the crystal is 25.0, while the estimated bending angle is 34.5 μrad. There is a significant discrepancy between the measured bending angle at injection and flat top energy, which is also confirmed by comparison with simulations shown in Fig. 15. The observed apparent variation of the crystal bending as a function of the beam energy is not yet understood, since there are not physics principle that could explain it. The present working hypothesis is an effect due to the miscut angle, which for this crystal is comparable to it bending angle. The miscut angle is the relative angle between the crystalline planes and the crystal surface that can reduce the effective length of the crystalline planes seen by channeled halo particles, thus reducing the deflection given to them. Improvements to the simulations code are on-going in order to properly take this effect into account and provide specifications on the miscut of future crystals.

Due to the trip of various power convertes of orbit correctors, the orbit of Beam 2 changed and it was not possible to perform reliable loss maps for cleaning measurements.

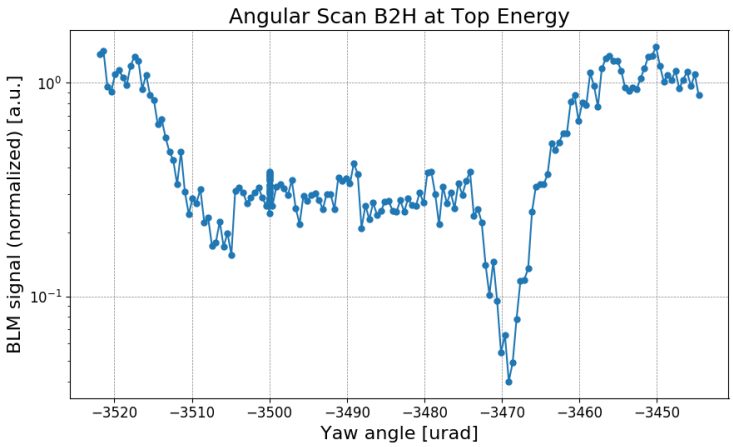

(a) Angular scan: normalized losses at the absorber as a function of the crystal angle.

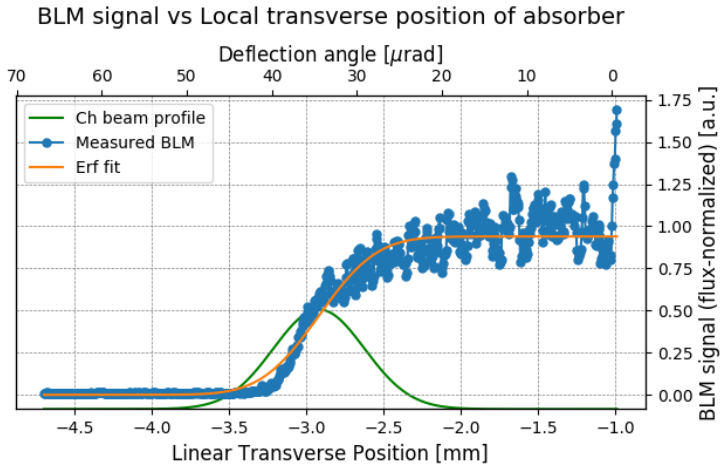

(b) Linear scan: normalized losses at the absorber as a function of its linear transverse position. An error function fit has been performed to estimate the deflection angle of the channeled beam.

Figure 14: Angular (top) and linear (bottom) scan on Beam 1 at flat top energy with the horizontal crystal (second MD block).

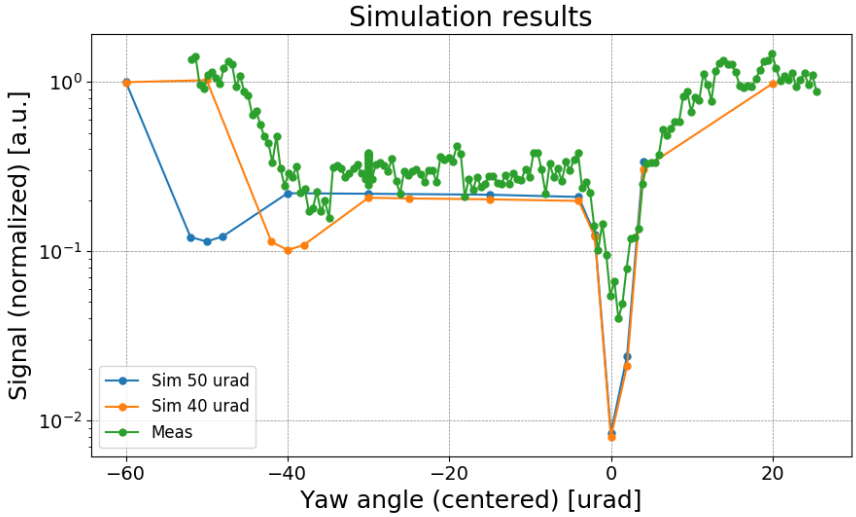

Figure 15: Comparison of measured B2H angular scan at top energy with simulations with a crystal bending angle of 50 and 40 μrad respectively (second MD block). The values are normalized to the amorphous level.

5 Acknowledgements

We would like to thank the OP crew for their assistance during the MD.

6 References

[1] D. Mirarchi, G. Hall, S. Redaelli, and W. Scandale, "Design and implementation of a crystal collimation test stand at the Large Hadron Collider," *The European Physical Journal C*, vol. 77, no. 6, p. 424, 2017.

[2] R. Rossi *et al.*, "Beam 2 crystal characterization measurements with proton beams in the LHC." CERN-ACC-NOTE-2018-0067.

[3] R. Rossi, *Experimental assessment of crystal collimation at the Large Hadron Collider*. PhD thesis, Università degli Studi di Roma "La Sapienza", 2017.

[4] R. Rossi *et al.*, "Crystal collimation with protons at injection energy." CERN-ACC-NOTE-2016-0035.

[5] R. Rossi *et al.*, "Crystal collimation with protons at flat top energy." CERN-ACC-NOTE-2017-0021.

[6] R. Rossi *et al.*, "Crystal collimation cleaning measurements with proton beams in LHC." CERN-ACC-NOTE-2018-0024.